Contribution from the Department of Structural Chemistry, University of Utrecht, Transitorium III, Utrecht, The Netherlands, and the Institute for Organic Chemistry TNO, Utrecht, The Netherlands

Crystal and Molecular Structure of 1,1,2,2-Tetrakis(pentacarbonylmanganio)-1,2-dibromoditin, a Transition Metal Substituted Ditin Compound

A. L. SPEK, K. D. BOS, E. J. BULTEN, and J. G. NOLTES*

Received July 29, 1975 AIC505592

The crystal and molecular structure of 1,1,2,2-tetrakis(pentacarbonylmanganio)-1,2-dibromoditin, $Br_2Sn_2[Mn(CO)_5]_4$, has been determined by a single-crystal x-ray analysis using three-dimensional x-ray data collected by the ω-scan technique on an Enraf-Nonius CAD4 automated diffractometer. The compound crystallizes in the monoclinic system with four molecules in a centrosymmetric unit cell, with space group $P2_1/c$ and lattice parameters a = 16.591 (5) Å, b = 12.455 (2) Å, c = 17.214 (8) Å, and β = 108.10 (3)°. The heavy-atom part of the structure was solved with a direct method. The other atoms were located by Fourier methods. A refinement by block-diagonal least-squares procedures converged to R_F = 0.048 and R_{wF} = 0.036 for 4396 independent observed reflections with $I > 2.5\sigma(I)$. The crystal structure consists of discrete molecular units of $Br_2Sn_2[Mn(CO)_5]_4$. The two connected tin atoms are each tetrahedrally surrounded by two $Mn(CO)_5$ groups and one bromine atom. Each manganese atom is octahedrally surrounded by five carbonyl groups and a tin atom. The four equatorial carbonyls in each $Mn(CO)_5$ group are bent away from the axial carbonyl group by 2.7° on the average. The internal steric crowding is decreased by the deformation of some Sn–Mn–C bond angles and Sn–Mn bond distances. The molecule exhibits approximate C_2 symmetry. Both the Sn–Sn bond length (2.885 (1) Å) and the Sn–Br bond lengths (2.576 (1) Å) are unusually long. The two Sn–Mn bond distances on each tin atom differ significantly by 0.040 (2) Å, with averages 2.747 (3) and 2.707 (3) Å. The average axial Mn–C distance is 1.829 (4) Å and the average equatorial Mn–C distance is 1.842 (3) Å. The mean C–O distance is 1.140 (2) Å.

Introduction

Numerous compounds containing a tin–transition metal bond have been synthesized.[1] The crystal and molecular structures of several of these compounds have been reported.[2] Also the crystal and molecular structures of several compounds containing a Sn–Sn bond are known.[3-6] We have recently reported examples of compounds containing a tin–tin bond as well as tin–transition metal bonds, viz., $H_2Sn_2[Mn(CO)_5]_4$ and $X_2Sn_2[Mn(CO)_5]_4$ with X = Cl, Br.[7,8] Our interest in the tetrakis(pentacarbonylmanganio)ditin dihydride and the corresponding dihalides stems from their potential usefulness as starting materials for the synthesis of linear polymers having backbones consisting of covalently bonded metal atoms. Such materials might conceivably display anisotropic electron transport properties (cf. also the recent synthesis of intermetallic oligomers employing transition metal substituted tin and germanium halides[9]). The crystal and molecular structure of $H_2Sn_2[Mn(CO)_5]_4$ has been published.[7,8] An interesting aspect of the structure is the distortion of the bonds around the tin atom from a tetrahedral structure. Both the bond lengths and the bond angles of the two Sn–Mn bonds differed significantly.

Unfortunately, it was not possible to determine the position of the hydrogen atoms in this structure because of the experimental difficulties encountered.

In order to assess more completely the bond lengths and bond angles around the tin atom in this class of compounds, we carried out an x-ray investigation of the corresponding dibromide $Br_2Sn_2[Mn(CO)_5]_4$.

Experimental Section

Crystal data for $Br_2Sn_2[Mn(CO)_5]_4$: monoclinic, space group $P2_1/c$, a = 16.591 (5) Å, b = 12.455 (2) Å, c = 17.214 (8) Å, β = 108.10 (3)°, V = 3381 Å^3, Z = 4, ρ(obsd) = 2.29 g cm^{-3}, ρ(calcd) = 2.31 g cm^{-3}, mol wt 1177.2; μ(Mo Kα) = 55.9 cm^{-1}, F(000) = 2216 electrons.

Transparent dark-red crystals of the title compound were obtained as described in ref 8.

A specimen that gave sharp optical extinctions under crossed polarizers was mounted along its macroscopic twofold axis (b axis). On the basis of a Weissenberg photograph ($h0l$) and two precession photographs ($hk0$ and $0kl$) the crystal was found to belong to the monoclinic system. The systematic absences observed ($0k0$ for $k = 2n + 1$ and $h0l$ for $l = 2n + 1$) indicate that the space group is $P2_1/c$, C_{2h}^5. The relatively high-temperature movement of the molecules was reflected in a fast drop of the intensities beyond $(\sin\theta)/\lambda$ = 0.5 Å^{-1}. At this point the crystal was remounted for data collection with the spindle axis approximately parallel to [101]. Accurate values of the unit cell parameters and the crystal orientation matrix were determined at ambient room temperature from a least-squares treatment of the angular settings of eight reflections, carefully centered on an Enraf-Nonius CAD4 computer controlled diffractometer using Mo Kα radiation (λ 0.71069 Å).[10] The standard deviations in the lattice parameters were obtained from the comparison of the deviations from integer values of the indexes, calculated with the orientational matrix, for the angular settings of the orientation reflections as described by Duisenberg.[11] The density calculated for four molecules in the unit cell agrees well with the value obtained by flotation in a mixture of dichloromethane and dibromomethane.

Collection and Reduction of the Intensity Data

The crystal selected for data collection was a regular parallelepiped with two additional small facets perpendicular to the alongated a direction. The observed crystallographic forms, indexed in accordance with the unit cell determined by x-ray diffraction, were $\{\bar{1}11\}$, $\{11\bar{1}\}$, $\{001\}$, and $\{100\}$. Dimensions were measured under a binocular microscope and were $(\bar{1}11)$ to $(1\bar{1}\bar{1})$ 0.18 mm, $(11\bar{1})$ to $(\bar{1}\bar{1}1)$ 0.25 mm, (001) to $(00\bar{1})$ 0.25 mm, and (100) to $(\bar{1}00)$ 0.40 mm. The crystal volume amounts to 1.41×10^{-2} mm^3.

Intensity data were collected with the CAD4 diffractometer equipped with a scintillation counter in the ω-scan mode using zirconium-filtered Mo Kα radiation. The applied scan angle was $\Delta\omega = 0.74 + 1.42(\tan\theta)°$. The background was measured in an additional scan area of $\Delta\omega/4°$ on both sides of the main scan and with the same scan speed. The intensity of every reflection was measured at the highest possible speed and then, if necessary, at a speed designed to achieve I_{min} counts above background. A maximum t_{max} seconds was placed on the measurement time. The horizontal and vertical detector aperture were 3 and 4 mm, respectively, and the distance from the crystal to the aperture was 174 mm. An attenuator would have been automatically inserted if a preliminary scan indicated a count rate greater than 50000 counts per sec^{-1} [10] but it was not necessary.

The reflection (200) was used as a standard reflection and its intensity was monitored every 50 reflections. Fluctuations in the standard were within 3% from the mean. There was no indication for decay during the measurement.

Reflection data were collected in two parts. The first part contains all accessible reflections within the limiting sphere up to θ = 15°, with I_{min} = 300 counts and t_{max} = 35 sec. The second part contains the asymmetric set of reflections with θ values ranging from 15 to 27.5°

* To whom correspondence should be addressed at the Institute for Organic Chemistry TNO.

(I_{min} = 600 counts and t_{max} = 70 sec).

The intensities of a total of 12532 reflections were measured. The net intensity was calculated with

$$I(\text{net}) = (\text{scale})(S - 2(L + R))/\text{npi}$$

where $(L + R)$ is the total background count, S the scan count, npi the ratio of the maximum possible scan speed to the applied scan speed, and (scale) a function of the time slowly varying around the value 1. The data were scaled to take into account short- and long-range fluctuations in the intensity, by interpolation in a polynomial of the third degree through eight neighboring measurement values of the standard reflection, in order to smooth out very short-term fluctuations in the intensity of the standard reflection. The standard deviation in the net intensity was calculated with

$$\sigma(I) = \frac{\text{scale}}{\text{npi}}(S + 4(L + R))^{1/2}$$

Absorption correction was performed with a Gaussian integration technique using a 5 × 7 × 8 grid. The observed absorption corrections were in the range from 2.22 to 3.54.

The equivalent reflections were averaged using

$$\bar{I} = \sum_i (I_i/\sigma_i^2)/\sum_i (1/\sigma_i^2)$$

$$\sigma(\bar{I}) = [1/\sum_i (1/\sigma_i^2)]^{1/2}$$

where I_i and σ_i are the intensity and the standard deviation of the ith equivalent diffraction. The resulting unique set contained 7764 reflections of which 4396 had intensities above background ($I > 2.5\sigma(I)$). A total of 2552 reflections of the type "unobserved" were in the range θ = 21–27.5°. The data were corrected for Lorentz and polarization factors (Lp). The $\sigma(I)$'s were converted to the estimated errors in the relative structure factors $\sigma(F)$ by

$$\sigma(F) = [(I + \sigma(I))/Lp]^{1/2} - (I/Lp)^{1/2}$$

Solution and Refinement of the Structure

Direct methods were used to locate the positions of the heavier atoms. The $|F_o|$'s were normalized to $|E_o|$'s by means of a modified Wilson-plot procedure which corrects for the effect of overall anisotropic motion.[12] Statistics on these data, with the theoretical values for centrosymmetric and noncentrosymmetric structures in parentheses, are $\langle|E|\rangle$ = 0.780 (0.798, 0.886), $\langle|E^2 - 1|\rangle$ = 0.986 (0.968, 0.736), $\langle(|E^2 - 1|)^2\rangle$ = 1.860 (2.000, 1.000), and $\langle(|E^2 - 1|)^3\rangle$ = 6.735 (8.000, 2.000).

The structure determination was initiated with a variant of the symbolic addition procedure.[13] A total of 434 reflections with $E >$ 1.88 were selected, from which 4000 sign relations were generated. Three origin-determining reflections were chosen by the program and another 25 reflections were assigned symbolic signs. All other signs were found by insertion of these starting signs, and the newly derived signs, in reliable sign relations. After this, 19 symbolic signs were eliminated on the basis of reliable sign relations. The resulting set of 64 solutions was then sorted according to the value $\sum_{h,k} s_h s_k s_{h+k} |E_h E_k E_{h+k}|$. A Fourier synthesis, calculated for the solution with the highest value for the criterion, showed the positions of the two tin, four manganese, and two bromine atoms. All predicted signs proved to be correct later on. Because of the high noise level induced by the predominant heavy-atom contribution to the large E's, it is usually not possible to detect the lighter atoms in a direct-method solution. The other atoms were located in a Fourier synthesis calculated with signs as derived from the heavy-atom structure. The structure was refined assuming anisotropic thermal motion for all the atoms by a block-diagonal least-squares procedure. Unit weights were applied in the preliminary stages of the refinement. The structure refinement converged to R_F = 0.048 and R_{wF} = 0.053.[14] Refinement was continued after the introduction of weights on the basis of counting statistics. The final R values for 4396 observed reflections are R_F = 0.048 and R_{wF} = 0.036. A total of 426 parameters including one scale factor were varied. All shifts were less than half of their standard deviations when refinement was stopped. The final positional and thermal parameters are tabulated in Tables I and II. The average deviation in an observation of unit weight, defined by $[\sum w(|F_o| - |F_c|)^2/(m - n)]^{1/2}$, was 1.34 as compared to the ideal value 1. The function $\sum w(|F_o| - |F_c|)^2$ was not significantly dependent either upon F_o or upon $(\sin\theta)/\lambda$, thereby indicating a correctly chosen weighting scheme. The R value for all reflections including the "unobserveds" was 0.077. Ninety-two "unobserved" reflections had $\Delta F > 3\sigma(F)$, but all ΔF's were less than $5\sigma(F)$. A final electron density difference Fourier synthesis revealed no significant residual electron density maxima, apart from some features less than 1 e Å^{-3} around the heavier atoms, indicating that the correction for absorption was not completely effective. Scattering factors for Br, Sn, and Mn were taken from ref 15. The values for C and O are those of Cromer and Mann.[16] Anomalous dispersion corrections for Sn, Mn, and Br were taken from a compilation by Rietveld.[17] All computer calculations were performed on a CDC CYBER-73 computer at the computer center of the University of Utrecht. Programs used in this structural analysis included the local programs CAD4TAPE (for handling of the diffractometer output by D. Kaas), ABS (for absorption correction by A. J. M. Duisenberg), ASYM (averaging to the unique data set by A. L. Spek), AUDICE (a direct-method procedure by A. L. Spek), ORTEP (thermal ellipsoid drawing by C. K. Johnson[18]), STEREO (for stereoscopic drawings by D. Kaas), and an extended version of the X-RAY SYSTEM (by Stewart et al.[19] and implemented by the Dutch X-RAY SYSTEM group) for most of the other calculations.

Table I. Final Positional Parameters for $Br_2Sn_2[Mn(CO)_5]_4$[a]

Atom	x	y	z
Sn(1)	0.798 89 (3)	0.378 09 (4)	0.234 69 (3)
Sn(2)	0.715 14 (3)	0.554 55 (4)	0.286 37 (3)
Br(3)	0.882 3 (1)	0.317 9 (1)	0.380 7 (1)
Br(4)	0.621 3 (1)	0.438 5 (1)	0.347 4 (1)
Mn(5)	0.917 3 (1)	0.442 9 (1)	0.163 2 (1)
Mn(6)	0.706 0 (1)	0.199 5 (1)	0.179 8 (1)
Mn(7)	0.811 6 (1)	0.661 1 (1)	0.420 2 (1)
Mn(8)	0.606 4 (1)	0.670 4 (1)	0.161 3 (1)
C(9)	0.997 4 (5)	0.485 2 (6)	0.117 7 (4)
C(10)	0.999 5 (5)	0.401 3 (5)	0.257 8 (4)
C(11)	0.915 8 (5)	0.573 6 (6)	0.212 2 (4)
C(12)	0.828 7 (5)	0.484 3 (6)	0.073 6 (5)
C(13)	0.911 5 (5)	0.307 6 (7)	0.119 2 (5)
O(14)	1.049 4 (3)	0.509 8 (5)	0.089 8 (3)
O(15)	1.053 2 (3)	0.378 8 (4)	0.315 8 (3)
O(16)	0.913 7 (4)	0.656 4 (4)	0.240 5 (3)
O(17)	0.775 6 (4)	0.514 1 (5)	0.018 4 (4)
O(18)	0.909 6 (4)	0.225 1 (5)	0.090 2 (4)
C(19)	0.708 8 (5)	0.171 4 (7)	0.286 2 (5)
C(20)	0.708 3 (4)	0.240 4 (6)	0.077 7 (4)
C(21)	0.651 8 (6)	0.073 8 (7)	0.140 3 (5)
C(22)	0.607 0 (5)	0.274 9 (7)	0.164 3 (5)
C(23)	0.809 9 (5)	0.135 4 (6)	0.205 0 (4)
O(24)	0.710 5 (4)	0.147 2 (5)	0.351 3 (3)
O(25)	0.709 5 (4)	0.266 9 (5)	0.015 1 (3)
O(26)	0.617 4 (4)	−0.002 9 (5)	0.114 5 (4)
O(27)	0.543 5 (4)	0.317 8 (5)	0.152 6 (4)
O(28)	0.874 8 (4)	0.094 6 (5)	0.222 5 (4)
C(29)	0.708 5 (6)	0.707 7 (7)	0.428 0 (5)
C(30)	0.909 7 (6)	0.598 1 (7)	0.411 3 (5)
C(31)	0.815 2 (5)	0.769 4 (6)	0.349 3 (4)
C(32)	0.802 2 (5)	0.544 7 (6)	0.484 8 (4)
C(33)	0.874 0 (5)	0.742 2 (6)	0.507 1 (4)
O(34)	0.646 5 (4)	0.734 9 (6)	0.436 3 (4)
O(35)	0.971 3 (4)	0.561 1 (5)	0.408 2 (4)
O(36)	0.818 5 (4)	0.837 2 (4)	0.306 0 (3)
O(37)	0.797 7 (4)	0.478 4 (4)	0.527 8 (3)
O(38)	0.912 8 (3)	0.796 4 (4)	0.557 8 (3)
C(39)	0.613 9 (5)	0.781 6 (6)	0.234 7 (4)
C(40)	0.533 6 (5)	0.747 3 (6)	0.077 8 (5)
C(41)	0.699 7 (5)	0.724 3 (6)	0.138 8 (4)
C(42)	0.606 9 (6)	0.553 7 (8)	0.096 4 (6)
C(43)	0.521 8 (6)	0.609 5 (8)	0.193 5 (7)
O(44)	0.618 0 (4)	0.852 9 (5)	0.276 9 (3)
O(45)	0.489 8 (4)	0.793 5 (5)	0.024 4 (3)
O(46)	0.756 5 (3)	0.758 4 (5)	0.123 6 (3)
O(47)	0.606 0 (5)	0.483 6 (6)	0.053 9 (4)
O(48)	0.465 8 (5)	0.577 0 (6)	0.213 4 (6)

[a] The estimated standard deviations in the least significant figures are given in parentheses here and in other tables.

Description and Discussion of the Structure

The crystal structure of 1,1,2,2-tetrakis(pentacarbonyl-

Table II. Final Anisotropic Thermal Parameters for $Br_2Sn_2[Mn(CO)_5]_4$[a]

Atom	$100u_{11}$	$100u_{22}$	$100u_{33}$	$100u_{12}$	$100u_{13}$	$100u_{23}$
Sn(1)	3.59 (5)	3.47 (5)	3.32 (5)	−0.11 (3)	0.79 (3)	−0.38 (4)
Sn(2)	3.61 (5)	4.02 (5)	3.32 (5)	−0.12 (3)	1.02 (3)	−0.45 (2)
Br(3)	5.87 (7)	5.99 (7)	4.10 (6)	−0.34 (5)	0.23 (5)	0.53 (4)
Br(4)	6.70 (8)	8.14 (8)	6.63 (7)	−2.41 (6)	2.92 (5)	0.11 (6)
Mn(5)	4.13 (8)	4.19 (8)	3.78 (8)	0.28 (6)	1.16 (6)	−0.08 (6)
Mn(6)	5.16 (9)	4.54 (9)	4.07 (8)	−0.97 (6)	1.05 (6)	−0.51 (6)
Mn(7)	4.68 (8)	4.23 (8)	3.40 (7)	−0.22 (6)	1.22 (6)	−0.43 (5)
Mn(8)	3.97 (8)	5.36 (9)	4.76 (8)	0.62 (6)	0.76 (6)	−0.05 (6)
C(9)	5.0 (5)	5.8 (5)	4.1 (4)	0.5 (4)	0.7 (4)	0.3 (4)
C(10)	4.7 (5)	3.5 (4)	5.1 (5)	0.1 (4)	1.3 (4)	0.1 (4)
C(11)	4.3 (5)	5.3 (5)	3.4 (4)	0.1 (4)	1.3 (4)	0.9 (4)
C(12)	5.1 (6)	4.7 (6)	5.8 (6)	−1.0 (5)	1.9 (5)	−0.7 (5)
C(13)	5.3 (6)	5.8 (7)	4.6 (5)	1.2 (5)	0.8 (5)	−0.5 (5)
O(14)	5.3 (4)	11.2 (5)	6.3 (4)	−0.4 (4)	3.1 (3)	0.4 (4)
O(15)	5.4 (4)	7.2 (4)	5.9 (4)	0.6 (3)	0.4 (3)	1.3 (3)
O(16)	9.3 (5)	4.2 (4)	5.6 (4)	0.7 (3)	2.8 (3)	−0.1 (3)
O(17)	8.1 (5)	8.0 (5)	7.4 (5)	−0.2 (4)	−2.0 (4)	1.5 (4)
O(18)	8.5 (5)	6.1 (5)	10.7 (6)	0.7 (4)	2.4 (4)	−3.6 (4)
C(19)	7.0 (7)	6.9 (7)	6.8 (6)	−3.1 (5)	2.6 (5)	−1.2 (5)
C(20)	3.6 (5)	4.1 (5)	5.0 (5)	0.3 (4)	−0.4 (4)	−1.4 (4)
C(21)	8.0 (7)	6.2 (6)	5.3 (6)	−1.3 (5)	0.4 (5)	−1.2 (5)
C(22)	5.2 (6)	7.4 (7)	6.2 (6)	−1.7 (5)	1.9 (5)	−2.0 (5)
C(23)	7.4 (6)	4.3 (5)	4.6 (5)	0.7 (5)	1.0 (5)	0.1 (4)
O(24)	11.9 (6)	13.2 (6)	5.3 (4)	−6.0 (5)	2.2 (4)	0.3 (4)
O(25)	8.8 (5)	8.9 (5)	3.8 (3)	−0.9 (4)	1.4 (3)	−0.4 (3)
O(26)	14.6 (7)	7.0 (5)	10.1 (6)	−5.7 (5)	1.2 (5)	−2.5 (4)
O(27)	5.2 (4)	12.9 (6)	10.9 (6)	0.0 (4)	2.0 (4)	−3.9 (5)
O(28)	10.1 (6)	9.1 (5)	8.0 (5)	4.8 (4)	0.7 (4)	0.4 (4)
C(29)	6.7 (7)	5.9 (6)	3.0 (5)	−0.2 (5)	0.5 (5)	0.3 (4)
C(30)	5.5 (6)	5.1 (8)	3.6 (5)	−1.6 (5)	1.6 (5)	−0.1 (4)
C(31)	5.3 (5)	5.6 (6)	3.3 (5)	−2.0 (4)	0.7 (4)	−0.8 (4)
C(32)	4.5 (5)	6.1 (6)	4.1 (5)	−0.0 (4)	1.2 (4)	−0.4 (4)
C(33)	5.0 (5)	4.2 (5)	4.1 (5)	1.0 (4)	1.3 (4)	−0.1 (4)
O(34)	5.1 (4)	12.9 (6)	6.9 (5)	2.7 (4)	1.9 (4)	0.2 (1)
O(35)	4.9 (4)	6.5 (4)	7.7 (4)	−0.4 (4)	2.4 (4)	−0.7 (3)
O(36)	8.4 (5)	6.2 (4)	6.3 (4)	−2.1 (3)	1.8 (3)	1.0 (3)
O(37)	9.4 (5)	7.2 (4)	5.8 (4)	−0.9 (4)	2.7 (4)	2.2 (3)
O(38)	6.8 (4)	6.1 (4)	5.3 (4)	−0.1 (3)	0.2 (3)	−2.3 (3)
C(39)	6.5 (6)	5.5 (6)	4.3 (5)	1.8 (5)	1.0 (5)	0.9 (4)
C(40)	4.9 (6)	6.4 (6)	5.4 (5)	0.8 (5)	−0.5 (4)	−1.7 (5)
C(41)	5.1 (6)	6.3 (6)	4.0 (5)	0.2 (5)	1.2 (4)	0.5 (4)
C(42)	6.7 (7)	7.2 (8)	5.7 (7)	1.4 (6)	0.1 (5)	0.2 (5)
C(43)	4.6 (7)	8.1 (8)	11.9 (9)	1.6 (6)	2.6 (6)	2.3 (7)
O(44)	10.9 (5)	7.2 (4)	6.4 (4)	2.9 (4)	1.9 (4)	−0.9 (3)
O(45)	6.8 (4)	9.3 (5)	6.4 (4)	2.0 (4)	−1.7 (3)	0.4 (4)
O(46)	5.8 (4)	13.0 (6)	5.7 (4)	−1.1 (4)	1.5 (3)	0.7 (4)
O(47)	12.3 (6)	8.3 (6)	9.1 (6)	1.4 (5)	2.0 (5)	−2.9 (4)
O(48)	6.1 (5)	12.3 (7)	24.6 (11)	1.8 (5)	6.4 (6)	6.5 (7)

[a] The thermal parameters are in the form $t = \exp[-2\pi^2 \Sigma_i \Sigma_j u_{ij} h_i h_j a_i^* a_j^*]$.

manganio) 1,2-dibromoditin consists of discrete $Br_2Sn_2[Mn(CO)_5]_4$ molecular units, which are mutually separated by normal van der Waals distances. The projection of the unit cell content on the *ac* plane is shown in Figure 1. A stereoscopic drawing of the molecule (see Figure 2) clearly illustrates the noncrystallographic C_2 symmetry. The adopted atomic numbering scheme along with the thermal vibrational ellipsoids is shown in an ORTEP drawing[18] (Figure 3). Interatomic bond distances and bond angles are given in Tables III and IV. Thermal motion corrections were not applied.

Figure 4 shows the Newman projections for the Sn–Sn and Sn–Mn bonds. The overall geometry of $Br_2Sn_2[Mn(CO)_5]_4$ is closely similar to that of the related compound $H_2Sn_2[Mn(CO)_5]_4$.[8] However, whereas the C_2 point group symmetry of the dihydride in the crystal is exact, it is only approximate here. The bond length between the two tin atoms (2.885 (1) Å) is comparable with the value found for the dihydride (2.894 (5) Å), but significantly greater than that in the cyclic hexamer of diphenyltin (2.78 Å)[4] and that in hexaphenylditin (2.770 (4) Å).[3] A Sn–Sn bond length of 2.475 Å has recently been reported for $(C_6H_5)_3Sn^{IV}$–$Sn^{II}NO_3$.[6] The conformation about the Sn–Sn bond in the dibromide resembles that in the dihydride, but the corresponding torsional angles differ by approximately 10°. The tin atoms are in a strongly distorted tetrahedral environment, with average bond angles ⟨Sn–Sn–Br⟩ = 95.5°, ⟨Sn–Sn–Mn⟩ = 115.1°, ⟨Mn–Sn–Mn⟩ = 119.2°, and ⟨Mn–Sn–Br⟩ = 103.4°. This is not uncommon for tin–transition metal compounds because in these compounds the tin–transition metal bond has a strong s character, with the remaining bonds accordingly having stronger p character (for a review see ref 2). The unusually low Sn–H frequency observed in the ir spectrum of the dihydride is in accordance with a high p character of the Sn–H bond.[8] The observed Sn–Br bond distance of 2.576 (1) Å is not only longer than the values for other transition metal–tin bromides (2.50 Å in $(\pi\text{-}C_5H_5)(OC)_2Fe$–$SnBr_3$[20] and 2.520 Å in $[(CO)_4Co]_3SnBr$[21]) but also longer than distances reported for various other types of tin–bromine compounds in the literature (2.44–2.55 Å[22]). The two tin–manganese distances on each tin atom differ significantly by 0.040 (2) Å. It appears that the differences in the bond lengths are related with the crowding around the $Mn(CO)_5$ fragments and with the conformation around the tin–manganese bonds (Figure 4). The averages over the two pseudo-related pairs

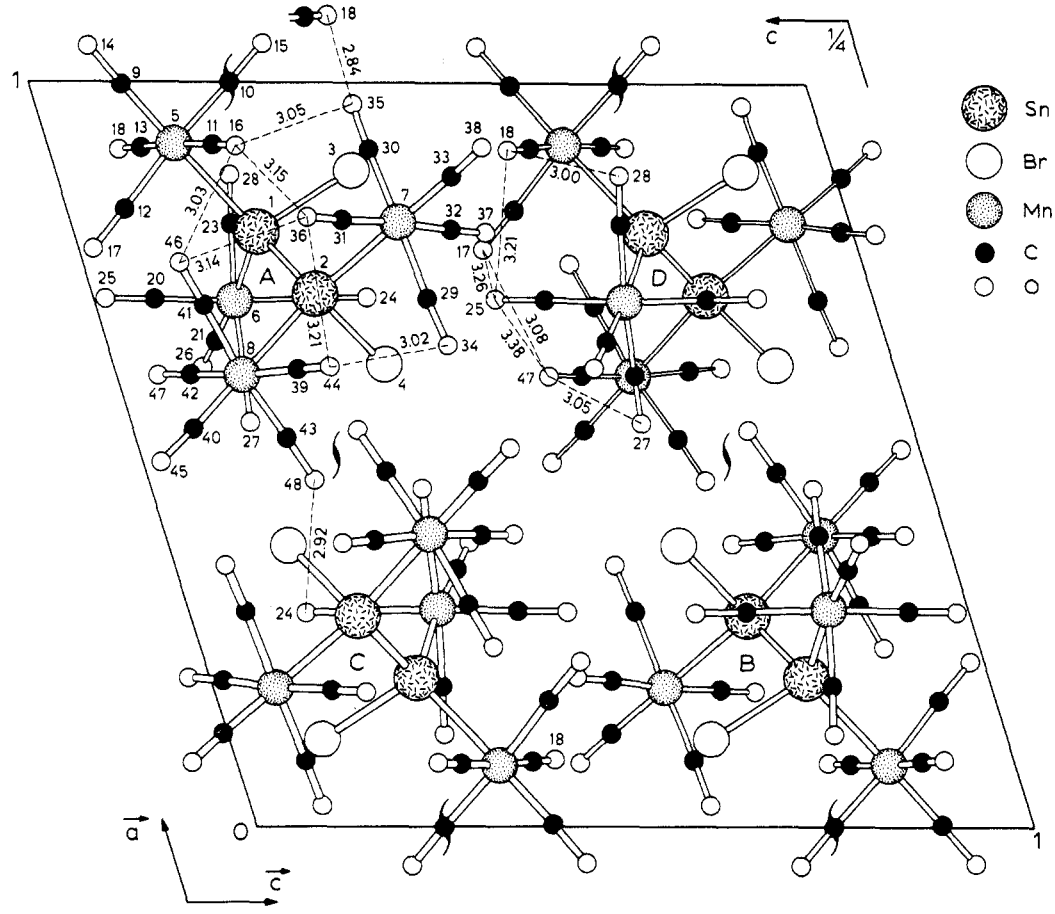

Figure 1. Packing of $Br_2Sn_2[Mn(CO)_5]_4$ molecules within the unit cell as viewed along the *b* axis. The molecules are at positions A = (x, y, z), B = ($1-x$, $1-y$, $1-z$), C = ($1-x$, $^1/_2+y$, $^1/_2-z$), D = (x, $^1/_2-y$, $^1/_2+z$).

Table III. Interatomic Distances (Å) for $Br_2Sn_2[Mn(CO)_5]_4$

Tin to Tin			
Sn(1)-Sn(2)	2.885 (1)		
Tin to Bromine			
Sn(1)-Br(3)	2.576 (1)	Sn(2)-Br(4)	2.576 (1)
Tin to Manganese			
Sn(1)-Mn(5)	2.743 (1)	Sn(2)-Mn(7)	2.709 (1)
Sn(1)-Mn(6)	2.704 (1)	Sn(2)-Mn(8)	2.750 (1)
Manganese to Axial Carbonyl Carbons			
Mn(5)-C(9)	1.818 (8)	Mn(7)-C(33)	1.835 (7)
Mn(6)-C(21)	1.828 (8)	Mn(8)-C(40)	1.834 (8)
		Av	1.829 (4)
Manganese to Equatorial Carbonyl Carbons			
Mn(5)-C(10)	1.844 (8)	Mn(7)-C(30)	1.856 (9)
Mn(5)-C(11)	1.837 (7)	Mn(7)-C(31)	1.832 (8)
Mn(5)-C(12)	1.843 (9)	Mn(7)-C(32)	1.863 (8)
Mn(5)-C(13)	1.838 (9)	Mn(8)-C(39)	1.853 (8)
Mn(6)-C(19)	1.851 (9)	Mn(8)-C(41)	1.836 (8)
Mn(6)-C(20)	1.842 (8)	Mn(8)-C(42)	1.835 (10)
Mn(6)-C(22)	1.838 (8)	Mn(8)-C(43)	1.826 (10)
Mn(6)-C(23)	1.825 (8)	Av	1.842 (3)
Mn(7)-C(29)	1.850 (9)		
Carbon to Oxygen			
C(9)-O(14)	1.152 (9)	C(30)-O(35)	1.137 (10)
C(10)-O(15)	1.147 (9)	C(31)-O(36)	1.139 (9)
C(11)-O(16)	1.146 (9)	C(32)-O(37)	1.127 (10)
C(12)-O(17)	1.139 (11)	C(33)-O(38)	1.133 (9)
C(13)-O(18)	1.139 (11)	C(39)-O(44)	1.136 (10)
C(19)-O(24)	1.152 (11)	C(40)-O(45)	1.135 (10)
C(20)-O(25)	1.133 (10)	C(41)-O(46)	1.136 (12)
C(21)-O(26)	1.131 (10)	C(42)-O(47)	1.136 (12)
C(22)-O(27)	1.142 (10)	C(43)-O(48)	1.157 (15)
C(23)-O(28)	1.143 (10)	Av	1.140 (2)
C(29)-O(34)	1.133 (11)		

of Sn–Mn bonds are 2.747 (3) and 2.707 (3) Å. These values are of the same order as found in $ClSn[Mn(CO)_5]_3$ (2.70–2.76 Å[23] but significantly longer than in $(C_6H_5)_3SnMn(CO)_5$ (2.67 Å[24]) and $(CH_3)_3SnMn(CO)_5$ (2.67 Å[25]). The corresponding Sn–Mn distances in the related dihydride structure are 2.67 and 2.73 Å.[8] From the available data concerning the covalent Sn–Mn bond it seems clear that the internuclear Sn–Mn separation varies relatively easily to meet the requirements of minimal internal steric hindrance. However, the observation that the short Sn(1)–Mn(6) and Sn(2)–Mn(7) bonds lie in more or less a cis arrangement with respect to Sn–Br on the adjacent tin atom whereas the long Sn(1)–Mn(5) and Sn(2)–Mn(8) bonds lie in more or less a trans arrangement suggests that electronic effects are involved as well. (We thank a referee for this suggestion.) Each manganese atom is octahedrally coordinated by five carbonyl groups and a tin atom. Literature values[23-26] for the Mn–C bonds range from 1.75 to 1.85 Å. The distances found in this analysis are within this range. The average Mn–C (axial) distance 1.829 (4) Å is somewhat shorter than the average Mn–C (equatorial) distance 1.842 (3) Å, but this difference, 0.013 (5) Å, is not statistically significant.[27] The same effect has been noticed in related compounds.[24,26] The four equatorial carbonyl groups of the $Mn(CO)_5$ group are bent away from the axial carbonyl group by 2.7° on the average. The same effect has been found in the crystal structures of $(CH_3)_3SnMn(CO)_5$[25] (5.7°) and $(C_6H_5)_3SnMn(CO)_5$[24] (3.3°). The inward bending is attributed to apical–equatorial C···C repulsion.[28] A point in favor of this explanation is the observation in this structure determination that the Mn–C–O geometry appears to be internally more constant with respect to the Mn–C(axial) bond than related to the Mn–Sn bond; e.g., the larger value for the

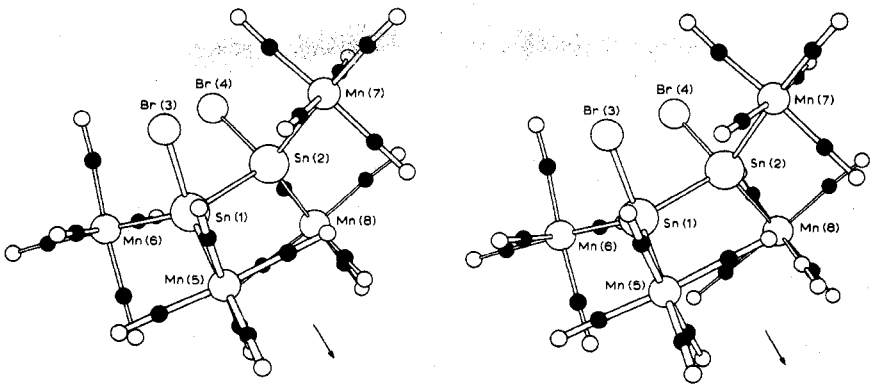

Figure 2. A stereoscopic drawing of $Br_2Sn_2[Mn(CO)_5]_4$. The noncrystallographic twofold axis of the molecule is indicated.

Table IV. Interatomic Angles (deg) for $Br_2Sn_2[Mn(CO)_5]_4$

Tin–Tin–Manganese			
Sn(1)–Sn(2)–Mn(7)	114.93 (3)	Sn(2)–Sn(1)–Mn(5)	113.26 (3)
–Mn(8)	114.85 (3)	–Mn(6)	117.26 (3)
Tin–Tin–Bromine			
Sn(1)–Sn(2)–Br(4)	96.21 (3)	Sn(2)–Sn(1)–Br(3)	94.88 (3)
Manganese–Tin–Manganese			
Mn(5)–Sn(1)–Mn(6)	119.66 (4)	Mn(7)–Sn(2)–Mn(8)	118.67 (4)
Bromine–Tin–Manganese			
Br(3)–Sn(1)–Mn(5)	106.32 (3)	Br(4)–Sn(2)–Mn(7)	101.58 (4)
–Mn(6)	100.18 (4)	–Mn(8)	106.35 (4)
Tin–Manganese–Carbon(Axial)			
Sn(1)–Mn(5)–C(9)	178.9 (2)	Sn(2)–Mn(7)–C(33)	175.9 (2)
–Mn(6)–C(21)	174.6 (3)	–Mn(8)–C(40)	179.7 (3)
Tin–Manganese–Carbon(Equatorial)			
Sn(1)–Mn(5)–C(10)	87.6 (2)	Sn(2)–Mn(7)–C(29)	84.3 (2)
–C(11)	86.6 (3)	–C(30)	91.4 (3)
–C(12)	87.8 (3)	–C(31)	85.8 (2)
–C(13)	87.8 (3)	–C(32)	89.4 (2)
Sn(1)–Mn(6)–C(19)	88.5 (3)	Sn(2)–Mn(8)–C(39)	88.2 (2)
–C(20)	85.8 (2)	–C(41)	88.1 (2)
–C(22)	91.0 (3)	–C(42)	86.3 (3)
–C(23)	83.3 (2)	–C(43)	85.6 (3)
Manganese–Carbon–Oxygen			
Mn(5)–C(9)–O(14)	178.2 (6)	Mn(7)–C(29)–O(34)	177.0 (7)
–C(10)–O(15)	176.8 (6)	–C(30)–O(35)	177.7 (7)
–C(11)–O(16)	178.0 (6)	–C(31)–O(36)	179.0 (6)
–C(12)–O(17)	177.0 (7)	–C(32)–O(37)	175.8 (6)
–C(13)–O(18)	177.5 (7)	–C(33)–O(38)	176.3 (6)
Mn(6)–C(19)–O(24)	175.7 (7)	Mn(8)–C(39)–O(44)	177.0 (6)
–C(20)–O(25)	179.1 (6)	–C(40)–O(45)	177.7 (7)
–C(21)–O(26)	178.6 (7)	–C(41)–O(46)	178.8 (6)
–C(22)–O(27)	176.8 (7)	–C(42)–O(47)	177.6 (8)
–C(23)–O(28)	178.4 (7)	–C(43)–O(48)	175.8 (8)
Carbon(Axial)–Manganese–Carbon(Equatorial)			
C(9)–Mn(5)–C(10)	91.3 (3)	C(33)–Mn(7)–C(29)	93.9 (4)
–C(11)	93.3 (3)	–C(30)	90.7 (4)
–C(12)	93.3 (4)	–C(31)	90.6 (3)
–C(13)	92.3 (4)	–C(32)	94.2 (3)
C(21)–Mn(6)–C(19)	93.7 (4)	C(40)–Mn(8)–C(39)	91.9 (4)
–C(20)	92.1 (3)	–C(41)	92.1 (4)
–C(22)	94.0 (4)	–C(42)	93.6 (4)
–C(23)	91.9 (4)	–C(43)	94.2 (4)
Carbon(Equatorial)–Manganese–Carbon(Equatorial)			
C(10)–Mn(5)–C(11)	87.4 (3)	C(39)–Mn(8)–C(41)	89.3 (4)
–C(13)	92.3 (4)	–C(43)	89.9 (4)
C(12)–Mn(5)–C(11)	90.9 (4)	C(42)–Mn(8)–C(41)	89.9 (4)
–C(13)	89.2 (3)	–C(43)	90.3 (5)
C(19)–Mn(6)–C(22)	89.3 (4)	C(10)–Mn(5)–C(12)	175.2 (4)
–C(23)	87.2 (4)	C(11)–Mn(5)–C(13)	174.4 (4)
C(20)–Mn(6)–C(22)	90.2 (4)	C(19)–Mn(6)–C(20)	174.2 (3)
–C(23)	92.9 (3)	C(22)–Mn(6)–C(23)	173.3 (3)
C(29)–Mn(7)–C(31)	92.6 (4)	C(29)–Mn(7)–C(30)	173.2 (4)
–C(32)	87.1 (4)	C(31)–Mn(7)–C(32)	175.2 (3)
C(30)–Mn(7)–C(31)	92.6 (4)	C(39)–Mn(8)–C(42)	174.5 (3)
–C(32)	87.6 (3)	C(41)–Mn(8)–C(43)	173.6 (4)

Table V. Least-Squares Planes[a] through the Equatorial Carbon Atoms of the $Mn(CO)_5$ Fragments

Atom	Dev from plane, Å	Atom	Dev from plane, Å
	Plane I		
C(10)	+0.0078	C(13)	−0.0077
C(11)	−0.0079	Mn(5)[b]	+0.0812
C(12)	+0.0077		
	Plane II		
C(29)	+0.0022	C(32)	−0.0023
C(30)	+0.0022	Mn(7)[b]	+0.0749
C(31)	−0.0021		
	Plane III		
C(19)	−0.0004	C(23)	+0.0004
C(20)	−0.0003	Mn(6)[b]	−0.0924
C(22)	+0.0004		
	Plane IV		
C(39)	−0.0065	C(43)	+0.0065
C(41)	+0.0065	Mn(8)[b]	−0.0951
C(42)	−0.0065		

Equations to Planes

I: $14.188x + 3.777y - 11.452z = 12.737$
II: $4.605x + 6.698y + 11.542z = 12.940$
III: $6.589x + 10.601y + 3.492z = 7.487$
IV: $7.118x - 6.274y + 9.974z = 1.8135$

[a] The planes are defined in fractional coordinates (x, y, z). [b] These atoms were given zero weight in the calculation of the least-squares plane. All other atoms were given unit weight.

Table VI. Selected Intramolecular Nonbonded Distances < 3.5 Å

Between the $Mn(CO)_5$ Fragments			
C(10)···O(35)	3.411	O(18)···C(20)	3.285
C(11)···C(30)	3.475	···C(23)	3.150
···O(35)	3.213	···O(25)	3.209
···O(46)	3.479	···O(28)	2.996
C(12)···O(25)	3.319	C(20)···O(47)	3.434
C(13)···C(20)	3.329	C(22)···O(47)	3.217
···C(23)	3.342	O(25)···O(47)	3.375
···O(25)	3.312	O(27)···C(42)	3.363
···O(28)	3.353	···O(47)	3.053
O(15)···O(35)	3.298	C(29)···C(39)	3.337
O(16)···C(30)	3.051	C(30)···O(44)	3.141
···C(31)	3.172	C(31)···C(38)	3.465
···O(35)	2.990	···C(39)	3.313
···O(36)	3.153	···C(44)	3.287
···O(46)	3.034	C(34)···C(39)	3.392
O(17)···O(25)	3.263	···C(44)	3.018
···C(42)	3.495	C(36)···C(39)	3.305
···C(47)	3.083	···C(41)	3.259
		···C(44)	3.212
		···C(46)	3.142
Between Br and C, O			
Br(3)···C(10)	3.448	Br(4)···C(32)	3.457
···O(15)	3.440	···C(43)	3.401
···C(19)	3.369	···O(48)	3.355
···O(24)	3.463		
···O(35)	3.338		

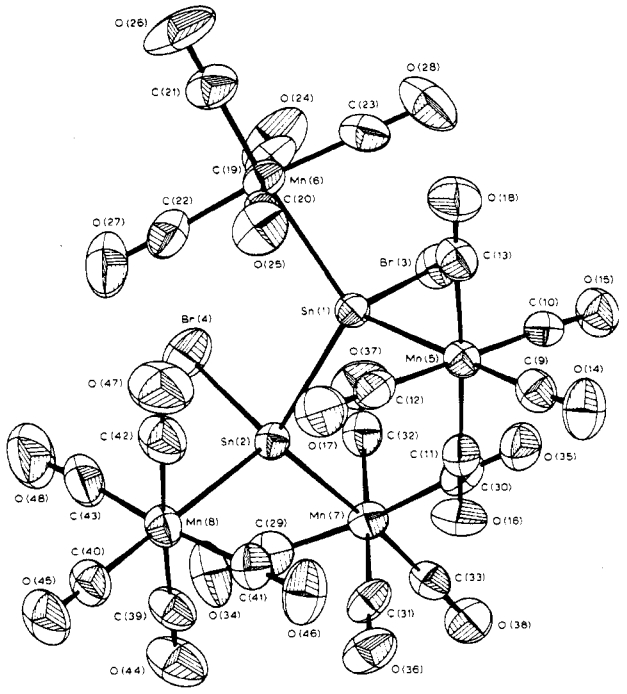

Figure 3. The 50% probability ellipsoids for $Br_2Sn_2[Mn(CO)_5]_4$. The adopted numbering scheme is indicated.

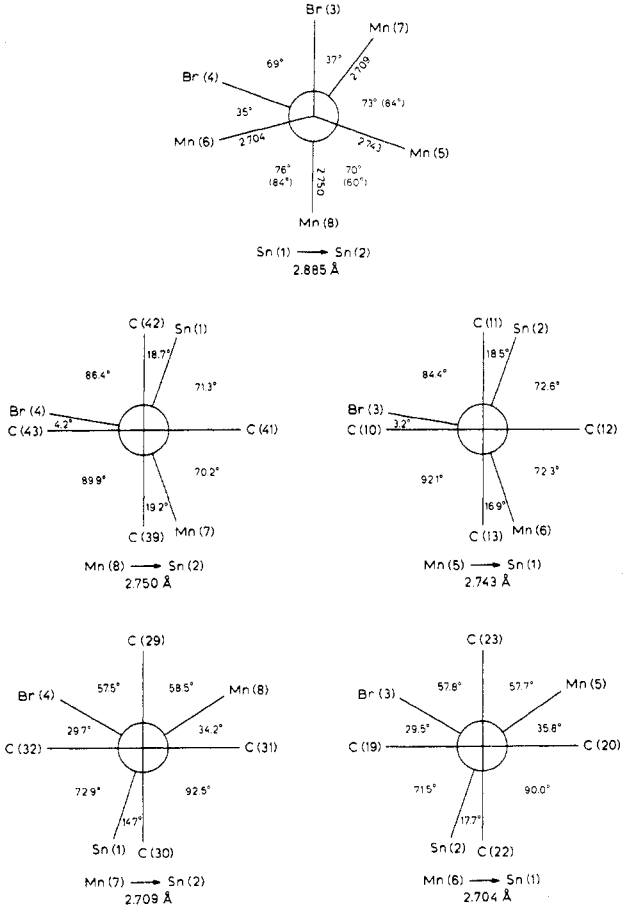

Figure 4. Newman projections along the Sn–Sn and Sn–Mn bonds. The corresponding values for the torsion angles around the Sn–Sn bond in $H_2Sn_2[Mn(CO)_5]_4$ are given in parentheses.

angle C(22)–Mn(6)–Sn(1) is compensated by the smaller C(23)–Mn(6)–Sn(1) angle.

Two of the C–Mn–Sn angles that are related by the pseudo-twofold symmetry are greater than 90°. This can probably be attributed to internal steric hindrance factors, as indicated by the internal symmetry relation. The four manganese atoms are displaced by 0.081, 0.092, 0.075, and 0.095 Å out of the corresponding least-squares planes, defined by the four carbonyl carbon atoms (see Table V). The mean C–O bond distance 1.140 (8) Å agrees well with the value 1.148 (12) Å in $(CH_3)_3Sn[Mn(CO)_5]$[25] and also with values observed in other transition metal carbonyls. There is no significant difference between the axial and equatorial C–O distances. Table VI gives a list of nonbonded intramolecular distances between atoms in different fragments that are related by at least one torsional degree of freedom. Table VII lists intermolecular distances. There are no abnormally short intermolecular contacts. The shortest O···O contact (2.84 Å) is larger than the sum of the van der Waals radii (2.8 Å[29]). The thermal parameters of the oxygens of the carbonyl groups are relatively high as is generally observed in this type of complex.

Table VII. Intermolecular Contacts Less Than 3.6 Å in Length between the Basic Molecule and Its Neighbors[a]

Molecule at $2-x, 1-y, -z$			
C(9)···O(14)	3.41	O(14)···O(14)	3.03
Molecule at $1-x, 1-y, -z$			
C(20)···O(45)	3.24	O(25)···O(45)	3.25
C(21)···O(45)	3.49	O(27)···O(45)	3.24
C(22)···O(45)	3.26	O(47)···O(47)	3.45
Molecule at $2-x, 1-y, 1-z$			
Br(3)···O(38)	3.53	O(15)···O(33)	3.28
O(15)···O(38)	3.01	O(35)···O(35)	3.37
O(15)···O(37)	3.52		
Molecule at $1-x, {}^1/_2+y, {}^1/_2-z$ $(1-x, -{}^1/_2+y, {}^1/_2-z)$			
O(48)···C(19)	3.13	O(34)···O(27)	3.22
O(48)···O(24)	2.92	O(44)···O(48)	3.15
O(44)···O(27)	3.30		
Molecule at $2-x, {}^1/_2+y, {}^1/_2-z$ $(2-x, -{}^1/_2+y, {}^1/_2-z)$			
C(9)···O(28)	3.21	O(16)···C(10)	3.37
C(10)···O(28)	3.13	O(36)···O(14)	3.19
C(11)···O(28)	3.31	O(36)···O(15)	3.46
O(14)···O(28)	3.26	O(46)···O(15)	3.36
O(15)···O(28)	3.09	O(16)···O(15)	3.04
O(16)···O(18)	3.54	O(30)···O(18)	3.40
O(16)···O(28)	3.45	O(35)···O(18)	2.84
O(36)···C(9)	3.46	O(37)···O(18)	3.13
Molecule at $x, {}^1/_2-y, {}^1/_2+z$ $(x, {}^1/_2-y, -{}^1/_2+z)$			
Br(3)···O(18)	3.53	O(24)···O(25)	3.02
O(24)···O(17)	3.40	O(37)···O(25)	3.36
O(37)···C(20)	3.34	O(37)···O(28)	3.32
O(37)···C(23)	3.31		
Molecule at $x, {}^3/_2-y, {}^1/_2+z$ $(x, {}^3/_2-y, -{}^1/_2+z)$			
C(29)···O(46)	3.24	O(38)···C(11)	3.10
C(33)···O(46)	3.20	O(38)···C(9)	3.09
C(34)···C(40)	3.51	O(38)···C(12)	3.12
O(34)···C(41)	3.36	O(38)···C(14)	3.24
O(34)···O(45)	3.41	O(38)···O(16)	3.20
O(34)···O(46)	3.17	C(33)···O(17)	3.48
O(38)···O(46)	3.21	O(38)···O(17)	3.20
Molecule at $x, 1+y, z$ $(x, -1+y, z)$			
C(45)···O(26)	3.36	C(40)···O(26)	3.39
C(44)···O(26)	3.32	C(39)···O(26)	3.40

[a] Equivalent position for the reverse order of the atoms is given in parentheses (when different).

Acknowledgment. The authors are indebted to Professor Dr. A. F. Peerdeman for critical reading of the manuscript, to Dr. A. J. M. Duisenberg for the data collection, and to Mr. J. Hulscher for taking the x-ray photographs. The investigations were supported in part (A.L.S.) by The Netherlands Foundation for Chemical Research (SON) with financial aid from The Netherlands Organization for Advancement of Pure Research (ZWO). The CAD4 diffractometer was put at our

disposal by the ZWO organization.

Registry No. $Br_2Sn_2[Mn(CO)_5]_4$, 56397-61-6.

Supplementary Material Available: Listing of structure factor amplitudes (32 pages). Ordering information is given on any current masthead page.

References and Notes

(1) E. H. Brooks and R. J. Cross, *Organomet. Chem. Rev., Sect. A*, **6**, 227 (1970).
(2) B. Y. K. Ho and J. J. Zuckerman, *J. Organomet. Chem.*, **49**, 1 (1973).
(3) H. Preut, H. J. Haupt, and F. Huber, *Z. Anorg. Allg. Chem.*, **396**, 81 (1973).
(4) D. H. Olson and R. E. Rundle, *Inorg. Chem.*, **2**, 1310 (1963).
(5) G. Bandoli, D. A. Clementi, and C. Panattozi, *Chem. Commun.*, 311 (1971).
(6) M. Nardelli, C. Pellizzi, and G. Pellizzi, *J. Organomet. Chem.*, **85**, C43 (1975).
(7) K. D. Bos, E. J. Bulten, J. G. Noltes, and A. L. Spek, *J. Organomet. Chem.*, **71**, C52 (1974).
(8) K. D. Bos, E. J. Bulten, J. G. Noltes, and A. L. Spek, *J. Organomet. Chem.*, **92**, 33 (1975).
(9) J. P. Colman, J. K. Hoyano, and D. W. Murphy, *J. Am. Chem. Soc.*, **95**, 3424 (1973).
(10) "CAD4-Users Manual", Enraf-Nonius, Delft, 1972.
(11) A. J. M. Duisenberg, Collected Abstracts of the First European Enraf-Nonius CAD4-Users Meeting, Paris, June 1974.
(12) E. N. Maslen, *Acta Crystallogr., Sect. A*, **22**, 945 (1967).
(13) A. L. Spek, Thesis, University of Utrecht, 1975.
(14) The function minimized was $\sum(w(|F_o| - |F_c|))^2$. The refinement was on F. The unweighted and weighted residuals are defined as follows: $R_F = (\sum||F_o| - |F_c||)/(\sum|F_o|)$; $R_{wF} = [(\sum w(|F_o| - |F_c|)^2)/(\sum|F_o|^2)]^{1/2}$.
(15) "International Tables for X-Ray Crystallography", Vol. III, Kynoch Press, Birmingham, 1962, p 202.
(16) D. T. Cromer and J. B. Mann, *Acta Crystallogr., Sect. A*, **24**, 321 (1968).
(17) H. M. Rietveld, Fysica Memo 153, RCN Petten, The Netherlands, 1966.
(18) C. K. Johnson, "ORTEP", Report ORNL-3794, Oak Ridge National Laboratory, Oak Ridge, Tenn., 1965.
(19) J. M. Stewart, G. J. Kruger, H. L. Ammon, C. Dickinson, and S. R. Hall, "X-RAY SYSTEM", Technical Report TR-192, The Computer Science Center, University of Maryland, College Park, Md., 1972.
(20) G. A. Melson, P. F. Stokely, and R. F. Bryan, *J. Chem. Soc. A*, 2247 (1970).
(21) R. D. Ball and D. Hall, *J. Organomet. Chem.*, **52**, 293 (1973).
(22) *Chem. Soc., Spec. Publ.*, **No. 11** (1958).
(23) J. H. Tsai, J. J. Flynn, and F. P. Boer, *Chem. Commun.*, 702 (1967).
(24) H. P. Weber and R. F. Bryan, *Acta Crystallogr.*, **22**, 822 (1967).
(25) R. F. Bryan, *J. Chem. Soc. A*, 696 (1968).
(26) M. L. Katcher and G. L. Simon, *Inorg. Chem.*, **11**, 1651 (1972).
(27) The standard deviation $\sigma(\bar{x})$ in the mean value $\bar{x}$ was calculated with $\sigma(\bar{x}) = [\sum(x_i - \bar{x})^2/(n(n-1))]^{1/2}$.
(28) L. F. Dahl and R. E. Rundle, *Acta Crystallogr.*, **16**, 419 (1963).
(29) L. Pauling, "The Nature of the Chemical Bond", 3rd ed, Cornell University Press, Ithaca, N.Y., 1960, p 260.

Contribution from the Department of Chemistry, Purdue University, West Lafayette, Indiana 47907, and from the Materials Physics Division, Atomic Energy Research Establishment, Harwell, Oxfordshire OX11 Ora, England

Crystal Structure of a Condensed Phosphatosilicate, Oxovanadium(IV) Diphosphatomonosilicate, $VO(SiP_2O_8)$

CATHERINE E. RICE,[1a] WILLIAM R. ROBINSON,*[1a] and BRUCE C. TOFIELD*[1b]

Received July 31, 1975 AIC505693

Crystals of oxovanadium(IV) diphosphatomonosilicate, $VO(SiP_2O_8)$, are tetragonal, space group $P4/ncc$, $a = 8.747$ (2) Å, $c = 8.167$ (2) Å, and $Z = 4$. By use of Patterson and Fourier techniques, the structure has been solved from 1289 symmetry-independent structure factors collected on an automated diffractometer and refined to a weighted R of 0.031. The structure is composed of V=O···V=O···V=O chains (d(V=O) = 1.591 (2) Å, d(V···O) = 2.492 (2) Å) lying along the fourfold axes with parallel $Si(PO_4)_2Si(PO_4)_2Si$ chains along the $\bar{4}$ axes. These chains are joined by oxygen atoms of the PO_4 groups which complete the distorted VO_6 octahedra. A given PO_4 group is bonded to two V atoms (d(P–O) = 1.492 (1) Å, d(V–O) = 1.977 (1) Å) and two Si atoms (d(P–O) = 1.572 (1) Å, d(Si–O) = 1.610 (1) Å). All dimensions within the vanadium–oxygen octahedron and the diphosphatosilicate chain are similar to those observed in related compounds.

Introduction

Oxovanadium(IV) diphosphatomonosilicate was recently prepared[2] and appeared to be the first well-characterized compound containing a stoichiometric arrangement of condensed silicate and phosphate tetrahedra. The substitution of P^V for Si^{IV} in silicates or of Si^{IV} for P^V in phosphates is not, in fact, common in minerals (see ref 2) although a number of synthetic phosphosilicates with the apatite[3,4] or eulytine[5] structures, where the tetrahedra are not linked to one another, have been prepared. A very few phosphosilicates where there are no phosphate–silicate links but where the phosphate and silicate tetrahedra are crystallographically distinguished have also been characterized.[6,7]

The ease of preparation of $VO(SiP_2O_8)$[2] indicates, however, that phosphosilicates in general are not necessarily unstable and the stoichiometry (X_3O_8) of the tetrahedrally coordinated anion sublattice indicated a possibly novel arrangement compared to known silicate or phosphate structures. We have, therefore, undertaken the determination of the crystal structure of $VO(SiP_2O_8)$ to discover the anionic arrangement and also that of the VO^{2+} moiety. The latter is of interest because a magnetic ordering transition was observed[2] in $VO(SiP_2O_8)$ at 2.5 K.

Experimental Section

$VO(SiP_2O_8)$ was first prepared from the chemical transport of $VO(PO_3)_2$[8] with iodine in a quartz tube. Single crystals may also be prepared by chemical transport with chlorine, and polycrystalline $VO(SiP_2O_8)$ is formed from the direct combination of $VO(PO_3)_2$ with SiO_2.[2] A wedge-shaped crystal was selected from a sample of $VO(SiP_2O_8)$ produced during an attempt to transport $VO(PO_3)_2$ with I_2 in a quartz tube. The wedge was a rectangular plate measuring 0.229 mm parallel to the c axis of the tetragonal unit cell and 0.142 mm parallel to the a axis. The thickness of the plate parallel to b ranged from 0.057 mm at one end to 0.028 mm at the other.

Crystal Data: $VO(SiP_2O_8)$, mol wt 1139.92, $a = 8.747$ (2) Å, $c = 8.167$ (2) Å, $V = 624.8$ Å^3, $Z = 4$, $d_{measd} = 2.9$ (1) g cm^{-3},[8] $d_{calcd} = 3.03$ g cm^{-3}, Mo Kα radiation, λ 0.71069 Å, μ(Mo Kα) = 24.0 cm^{-1}; space group uniquely determined as $P4/ncc$ (No. 130) from diffraction symmetry and systematic absences ($hk0$, $h + k = 2n$; $0kl$, $l = 2n$; hhl, $l = 2n$).

Data Collection. The crystal was mounted along the long dimension. Weissenberg and precession photographs confirmed the space group